

# Applying Appearance Standards to Light Reflection Models

Harold B. Westlund\*

Gary W. Meyer†

Department of Computer and Information Science  
University of Oregon  
Eugene, OR 97403

## Abstract

Appearance standards for gloss, haze, and goniochromatic color are applied to computer graphic reflection models. Correspondences are derived between both the gloss and haze standards and the specular exponent of the Phong model, the surface roughness of the Ward model, and the surface roughness of the Cook-Torrance model. Metallic and pearlescent colors are rendered using three aspecular measurements defined in a proposed standard for goniochromatic color. The reflection models for gloss and goniochromatic color are combined to synthesize pictures of clear coated automotive paint. Advantages of using appearance standards to select reflection model parameters include the small number of required measurements and the inexpensive commercially available instruments necessary to acquire the data. The use of a standard appearance scale also provides a more intuitive way of selecting the reflection model parameters and a reflection model independent method of specifying appearance.

**CR Categories:** I.3.3 [Computer Graphics]: Picture/Image Generation; I.3.7 [Computer Graphics]: Three-Dimensional Graphics and Realism—*Color, shading, shadowing, and texture*;

**Keywords:** color, optics, reflection and shading models, rendering

## 1 Introduction

The appearance of an object is important in both the real world and in a computer graphic scene. From an object's color alone we can determine the season by the leaves, the weather by the sky, and the freshness of meat sold in the market. Gloss reveals to us the age of a car, the cleanliness of a table, and the quality of sushi. These judgments are made instinctively by analyzing the light reflected from the items to our eyes. When applied to synthetic imaging, we judge the realism of a computer graphic picture by the appearance of the objects in the rendered environment. If the light that reaches us from the image evokes a visual response similar to that of viewing the real world scene, we describe the picture as being realistic.

How an object looks has been recognized to be important by workers in both the field of computer graphics and the appearance industry. The reaction by computer graphics researchers has been

to develop increasingly general models of surface reflection and to build ever more sophisticated reflection measurement devices. This has ultimately led to the use of the complete Bidirectional Reflection Distribution Function (BRDF) to represent reflection [24] and to the measurement of a BRDF by the use of a spectrogoniophotometer [41]. The approach taken by appearance industry professionals has been completely different. They have tried to determine the minimum number of measurements necessary to characterize the largest possible set of practical appearance problems. This has produced one-dimensional scales of appearance, such as gloss, and inexpensive appearance measurement devices, such as glossmeters.

The quantification of appearance by the paint and coatings industries has resulted in a set of appearance measurement standards. Tristimulus colorimetry, which is essentially a measure of diffuse reflection color, is one example with which computer graphics professionals are already very familiar. However gloss, a measure of the magnitude of the specular reflection, and haze, which captures the width of the specular lobe, are both almost unknown terms within the computer graphics community. Gloss and haze demonstrate the critical importance, for appearance measurement, of knowing how much light is reflected within just a few degrees of the specular direction. Even when the magnitude and color of the reflected light change over the entire reflectance hemisphere, appearance professionals have learned that in many cases, such as automotive metallic and pearlescent paint, only a few key measurements are necessary. Finally, the measurement of gloss, haze, metallic paint and other standardized appearance parameters can all be accomplished with relatively inexpensive measurement instruments.

This paper applies existing appearance standards and simple appearance measurements to realistic image synthesis. Given existing computer graphic reflection models such as the Phong model, the Ward model and the Cook-Torrance model, a correspondence is developed between the parameters of these models and appearance measurement scales such as gloss and haze (Section 2). This provides an appearance based rational and a simple measurement scheme for setting the parameters of these models. A reflectance model is also presented for use with so-called goniochromatic surfaces such as metallic and pearlescent automotive paint (Section 3). This demonstrates that even complex surface reflection can often be captured with a few key measurements. Finally, the gloss based reflection models are combined with the goniochromatic reflection model to render, using as few as four data values, a clear-coated automotive surface finish (Section 4).

## 2 First Surface Reflection - Gloss and Haze

Upon cursory examination, gloss is a rather simple surface appearance attribute; a surface is either glossy or matte. However the subtleties of gloss which are missed on this conscious examination are easily captured by the subconscious. These subtleties indirectly tell us whether a shirt is satin or nylon and inform us that it's time

---

\*westlund@cs.uoregon.edu

†gary@cs.uoregon.edu

to clean the bathroom mirror. These are the same subtleties that have pushed industry to come up with ways to both quantify and to measure gloss.

## 2.1 Current Standards

Gloss is defined by the American Society for Testing and Materials (ASTM) to be “the angular selectivity of reflectance, involving surface-reflected light, responsible for the degree to which reflected highlights or images of objects may be seen as superimposed on a surface” [5]. The seminal work on gloss measurement was performed by Hunter beginning in the 1930s. This work led him in 1937 to the differentiation of no less than six types of gloss: specular gloss, sheen, contrast gloss (or luster), absence-of-bloom gloss, distinctness of image gloss, and surface-uniformity gloss [21]. Categorizing gloss helped to quantify its subtleties and led to the first standardized measurement of gloss, ASTM method D523-39, Test for Specular Gloss [23]. This standard method, which survives actively to this day, measures the light reflected in the specular direction off the sample surface, 60 degrees down from surface normal. A surface of high gloss will reflect most light in the specular direction while a surface with low gloss (e.g., a Lambertian surface) will reflect most of its light in directions other than specular. The numerical gloss value,  $G$ , assigned to a surface typically ranges from 100 (high gloss) to 0 (low gloss).

A primary goal in establishing standard gloss measurements is to create an instrument measurement with a scale that mimics the numerical appraisal of an appearance professional. Because of the wide range of gloss values it was found that the correlation between gloss values for the 60 degree specular gloss meter and equivalent human assigned values were valid for too small a range of glossiness. Better correlation for specular gloss was achieved by adding two more instruments, one which measured specular gloss at grazing angles (termed sheen by Hunter) and another which measured specular gloss at near normal angles. These two measurements now are also part of ASTM D523, which assigns the angles from normal to be 85 degrees and 20 degrees respectively. Results have confirmed that the 20, 60 and 85 degree specular gloss measurements offer numerical values which are roughly linearly correlated over a range of values to perceived gloss of high-gloss, medium-gloss, and low-gloss surfaces respectively [22]. Figure 1 shows a graphical comparison of measured to perceived gloss for different specular gloss standards.

Pellacini, Ferwerda, and Greenberg [32] have pointed out some of the limitations of the existing ASTM gloss standard. They have taken on the important task of developing an improved definition of gloss and of applying it to computer graphics. However, the ASTM standard is still widely and successfully employed in the appearance industry, and there are inexpensive commercial instruments available that can be used to make ASTM standard gloss measurements. Thus there are compelling reasons to also utilize the current ASTM gloss standard in computer graphics.

Among other standards that are important to industry are haze and distinctness-of-image gloss measurements specified in ASTM E430, test method A [6]. These measurements compare the light reflected directly in the specular direction to that reflected in the slightly off-specular direction. For distinctness-of-image gloss, the angle of offset is essentially “as close as we can get” – centered a mere 0.3 degrees off of specular. This is to mimic the keen discrimination the human visual system has for detecting the sharpness of the reflection of an object in a highly reflective surface [22]. The quantity measured is  $G_{doi}$  which varies as with specular gloss; a larger value of  $G_{doi}$  corresponds to a more distinct image (i.e., a higher gloss value). The two haze measurements specified in ASTM E430 offer better correlation to the perceived haziness of surfaces with more directionally diverse surface scatter. The haze

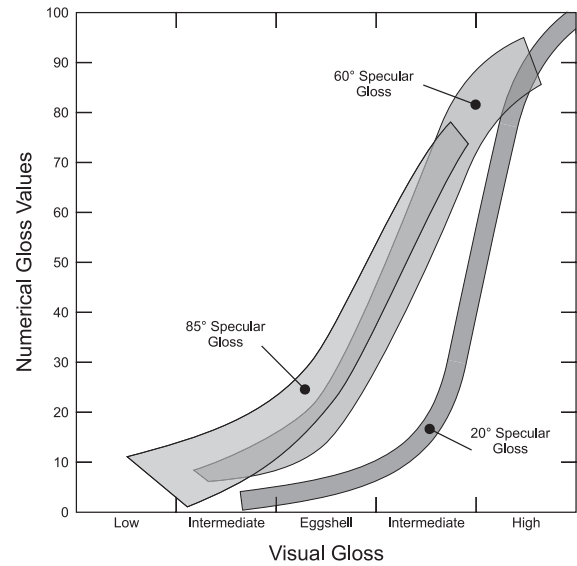


Figure 1: Numerical gloss values vs. visual gloss rating for ASTM specular gloss standards (after Hunter and Harold [22]). The thickness of each curve denotes the variance in the the sample observations.

value is a measure of the similarity between the pure specular reflection (measured with 30 degree gloss) and off-specular reflection (measured either 2 or 5 degrees off specular). One more haze measurement is specified in ASTM D4039 [3], which utilizes the difference between the 20 and 60 degree specular gloss measurements. This haze measurement takes advantage of the difference in the sizes of detector apertures of the two gloss measurements to measure specular and off-specular reflection. The convention used for the measured value of haze,  $H$ , is an increasing numerical value associated with increasing haziness.

A more detailed list of the above standards specifications is listed in Figure 2. The ASTM provides a complete description of all these standards, updated annually [2]. An excellent overview of these appearance measurement standards is offered by Hunter and Harold [22]. In addition, this text includes a discussion of other appearance based standards relating to specific industries.

## 2.2 Virtual Light Meter

The measure of gloss is a simplification of the BRDF down to a single appearance related quantity. Using a BRDF model as the representation of light reflection in computer graphics affords subtle appearance detail but also presents difficulty in selecting the correct BRDF model parameters. What is necessary is a way to develop a correspondence between BRDF model parameters and standard appearance measurements. A virtual light meter was constructed for this purpose. In the same way that various gloss meters give control over surface reflection properties to the product engineer, a virtual light meter can give control over BRDF model parameters to the computer graphics appearance designer.

The virtual light meter is essentially a customized integration tool, using numerical quadrature of the specified BRDF model over an adaptively subdivided source and receptor aperture (Figure 3) to compute the final standard appearance value. In addition to being able to calculate the standards (specular gloss, haze, and distinctness-of-image) the virtual light meter can be customized for other measurements. The customizable parameters include the size and locations of the source and receptor apertures, the specular an-

Gloss	ASTM Standard	Specular Angle	Aspecular Angle	Aperture Field (in degrees)	
				Source	Receptor
Specular gloss	D523	20°	0°	0.75 × 2.5	1.8 × 3.6
Specular gloss	D523	60°	0°	0.75 × 2.5	4.4 × 11.7
Specular gloss (sheen)	D523	85°	0°	0.75 × 2.5	4.0 × 6.0
Specular gloss	E430	30°	0°	0.44 × 5.0	0.4 × 3.0
Distinctness-of-image	E430	30°	±0.3°	0.44 × 5.0	0.14 × 3.0
Haze	E430	30°	±2°	0.44 × 5.0	0.4 × 3.0 or 0.5 × 3.0
Haze	E430	30°	±5°	0.44 × 5.0	0.4 × 3.0 or 0.5 × 3.0

Figure 2: Standard gloss and haze measurement specifications (after Hunter and Harold [22]). Specular and aspecular angles are measured in the plane of incidence. Aperture fields are measured as (in plane of measurement) × (perpendicular to plane of measurement). Values are taken from ASTM [4, 6]. See Figure 3 below for a diagram of 60 degree specular gloss.

gle, the surface orientation, and the reflection model.

Gloss values are directly dependent upon the measured flux reflected off the surface and passing through the receptor aperture. The integration of this flux begins by subdividing the source aperture. For each sample point on the source, the receptor aperture is subdivided. Based on the initial results of the integration, the receptor aperture is adaptively subdivided until the discretely computed flux is within some specified tolerance. Figure 3 shows an example of the flux due to one subdivided source element passing through the receptor. After this flux is determined, the next source sample point is chosen and the process is repeated. The source aperture continues to be subdivided until a specified tolerance is achieved. More detail of the integration process is offered below.

This virtual light meter allows the user to determine the specular gloss, distinctness-of-image, haze, etc. produced by a BRDF model with specified parameter values. To find the BRDF model parameters required to achieve a desired appearance value, the program can be run several times using different BRDF parameter values. Interpolation can then be used to compute the BRDF parameters required to achieve a desired gloss or haze value.

### 2.3 The Integration Method

To perform the integration over source and receiver apertures, the numerical cubature library tool Cubpack++ was used. Cubpack++ is an extensive C++, template based, class library for adaptive numerical integration of functions over two-dimensional areas [15, 16, 17, 18].

The rectangularly defined source and detector apertures are both subdivided adaptively by Cubpack++. Integration over the aperture which exists in world 3D space is achieved by coordinate transformation to local (i.e., aperture) 2D space. The rectangular ASTM definition of the aperture is particularly convenient for use in this cubature library since rectangles are primitive integration geometries. The surface irradiance due to each subdivided element of the source is modified by the sample BRDF and geometric conditions to find the flux at each detector patch. Rather than using the flux directly, we will discuss the integration process with respect to radiant exitance, the exitant flux density:

$$M \equiv \frac{d\Phi}{dA}$$

The irradiance at surface element  $dA$  due to  $S_j$ , the  $j^{th}$  patch of

the source aperture, is

$$dE_{S_j} = L_S \hat{s}_j \cdot \hat{n} d\omega_{S_j} \quad (1)$$

where  $L_S$  is the radiance of the source,  $\hat{s}_j$  is the unit direction vector of  $S_j$ ,  $\hat{n}$  is the unit normal vector to  $dA$ , and  $d\omega_{S_j}$  is the solid angle subtended by  $S_j$  at  $dA$ . The resulting surface radiance is the product of this irradiance and  $\rho(\hat{s}_j; \hat{r})$ , the BRDF of the surface:

$$dL(\hat{s}_j; \hat{r}) = \rho(\hat{s}_j; \hat{r}) dE_{S_j} \quad (2)$$

where  $\hat{r}$  is the unit direction vector of the exitant radiance. The radiant exitance can then be found at  $D_k$ , the  $k^{th}$  patch of the detector aperture by choosing the exitant direction of radiance to be the direction of the detector patch.

$$d^2 M_{S_j, D_k} = dL(\hat{s}_j; \hat{d}_k) \hat{d}_k \cdot \hat{n} d\omega_{D_k} \quad (3)$$

or

$$d^2 M_{S_j, D_k} = \rho(\hat{s}_j; \hat{d}_k) L_S \hat{s}_j \cdot \hat{n} d\omega_{S_j} \hat{d}_k \cdot \hat{n} d\omega_{D_k} \quad (4)$$

where  $\hat{d}_k$  is the unit direction vector of  $D_k$  and  $d\omega_{D_k}$  is the solid angle subtended by  $D_k$  at  $dA$ .

In order to simplify notation, it is common to write surface energy equations in terms of the projected solid angle [30] rather than the solid angle. Doing so, equation 4 becomes

$$d^2 M_{S_j, D_k} = \rho(\hat{s}_j; \hat{d}_k) L_S d\Omega_{S_j} d\Omega_{D_k} \quad (5)$$

where  $d\Omega_{S_j}$  and  $d\Omega_{D_k}$  are the projected solid angles of the source and detector patches respectively.

The total radiant exitance passing through the detector is then the double integral of  $d^2 M_{S_j, D_k}$  over both apertures. We approximate this by using the double sum and selecting an appropriately high subdivision for each aperture.

$$M_{S, D} = \sum_{k=1}^K \sum_{j=1}^J \rho(\hat{s}_j; \hat{d}_k) L_S d\Omega_{S_j} d\Omega_{D_k} \quad (6)$$

The source radiance,  $L_S$ , is constant so this can be brought out of the double sum:

$$M_{S, D} = L_S \sum_{k=1}^K \sum_{j=1}^J \rho(\hat{s}_j; \hat{d}_k) d\Omega_{S_j} d\Omega_{D_k}. \quad (7)$$

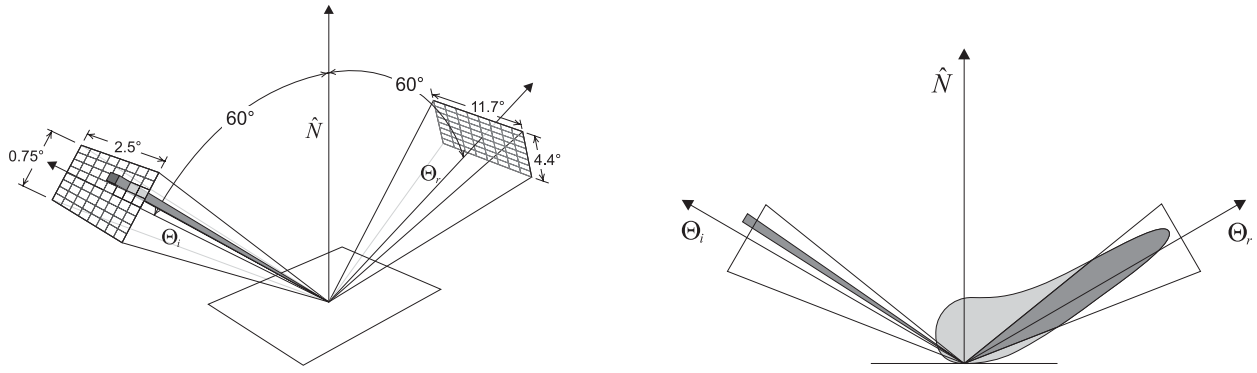


Figure 3: (left) Subdivision of light meter apertures using the 60 degree specular gloss specifications listed in Figure 2. The source and receptor apertures are oriented in directions  $\Theta_i$  and  $\Theta_r$ , 60 degrees down from the surface normal,  $\hat{N}$ , in the plane of incidence. (right) Flux passing through receptor aperture due to one source aperture subdivision. Aperture sizes are not to scale.

We now make the assumption that the radiant exitance is constant over the total illuminated surface area  $A$ . With this assumption, the total exitant flux passing through the detector aperture is:

$$\begin{aligned}\Phi_{S,D}(\rho) &= A M_{S,D} \\ &= A L_S \sum_{k=1}^K \sum_{j=1}^J \rho(\hat{s}_j; \hat{d}_k) d\Omega_{S_j} d\Omega_{D_k}\end{aligned}\quad (8)$$

The BRDF,  $\rho$ , is explicitly listed as parameter of  $\Phi$  to add clarity for when we later compare the exitant flux resulting from different surfaces.

## 2.4 Deriving Gloss Values

We now give an example of how the flux computed from the previous sub-section can be used to find a numerical standard gloss value. The gloss value chosen for discussion is the specular gloss, but similar techniques are used to derive the other gloss values.

The specular gloss defined by ASTM D523 is

$$G = 100 \frac{\Phi_{S,D}(\rho_{sample})}{\Phi_{S,D}(\rho_{standard})}\quad (9)$$

The standard surface is smooth black glass with a refractive index of 1.567. The blackness limits the exitant flux to that which is produced from first surface reflection while the smoothness ensures that the reflection is all in the specular direction. The BRDF of the standard is thus a function of the Fresnel reflectivity and a delta function:

$$\rho_{standard}(\hat{s}_j; \hat{d}_k) = \frac{F(n, \hat{s}_j) \delta(\text{mirror}(\hat{s}_j) - \hat{d}_k)}{d\Omega_{D_k}}\quad (10)$$

where  $F$  is the Fresnel reflectivity for unpolarized light,  $n$  is the refractive index of the standard, and  $\text{mirror}(\hat{s}_j)$  is the unit mirror direction vector of  $\hat{s}_j$ . The mirror direction vector can be computed with:

$$\text{mirror}(\hat{s}_j) = 2(\hat{s}_j \cdot \hat{n}) \hat{n} - \hat{s}_j.\quad (11)$$

The delta function is:

$$\delta(\bar{v}) = \begin{cases} 1 & \text{if } |\bar{v}| < \epsilon, \\ 0 & \text{if } |\bar{v}| \geq \epsilon. \end{cases}$$

Using (8) gives the flux reflected from the standard:

$$\begin{aligned}\Phi_{S,D}(\rho_{standard}) &= A L_S \sum_{k=1}^K \sum_{j=1}^J F(n, \hat{s}_j) \delta(\text{mirror}(\hat{s}_j) - \hat{d}_k) d\Omega_{S_j}\end{aligned}\quad (12)$$

This is computed off line and stored as a constant, for efficiency. If, however, a customized light meter specification utilized variable parameters, the standard flux value could easily be computed at run time.

Lastly, the computed flux of the sample and the standard are applied to (9) to determine the specular gloss value:

$$G = 100 \frac{\sum_{k=1}^K \sum_{j=1}^J \rho(\hat{s}_j; \hat{d}_k) d\Omega_{S_j} d\Omega_{D_k}}{\sum_{k=1}^K \sum_{j=1}^J F(n, \hat{s}_j) \delta(\text{mirror}(\hat{s}_j) - \hat{d}_k) d\Omega_{S_j}}.\quad (13)$$

As is expected, the sample area and source radiance drop out of the equation of gloss; specular gloss becomes a function of BRDF, index of refraction and geometry.

## 2.5 Utilizing Gloss and Haze

Using a virtual light meter avoids some of the pitfalls of real light meters. Unlike a real world surface, a virtual surface modeled with an analytical BRDF doesn't have imperfections or variations to be concerned about. Whereas a real surface may have curves or macroscopic height variations, its mathematical counterpart can be assured to be perfectly flat. Also, by having precise mathematical definitions with defined tolerances, the virtual light meter avoids real world manufacturing and thus avoids variances between light meters.

While the analytical nature of the virtual light meter circumvents several real world difficulties, the same computational scheme can become problematic when used in the evaluation of a physically based measurement such as gloss. Real world surfaces are dominated by Fresnel effects, but this is not necessarily so with BRDF models. Gloss and haze meters are designed to utilize these Fresnel effects in measurements. For analytical BRDF models not utilizing Fresnel reflectance, the ASTM gloss measurements of 20, 60 and 85 degrees will generally produce variance only because of the variance of the receptor aperture size. Other potential conflicts exist regarding characteristics of physically implausible BRDFs such as lack of energy conservation and lack of reciprocity as discussed by Lewis [27] and Shirley [40]. There are still advantages to the

simplification of these BRDFs down to a gloss or haze values, but the limitations must be kept in mind.

Several of the standard gloss measurements were computed for three reflection models as shown in Figures 4 to 6. Figure 4 relates specular gloss and haze to variation in the specular exponent for the Phong model [33] as modified by Lewis [27]. Lewis' modification scales the specular coefficient with a function of the specular exponent. Specular gloss and haze are displayed in Figures 5 and 6 as varying with surface roughness respectively for the Ward [26] and Cook-Torrance [14] reflection models.

As previously mentioned, the ASTM gloss and haze measurements are designed to work with surfaces exhibiting Fresnel effects. Any BRDF model which includes Fresnel reflection can be used without modification in the virtual haze and gloss meter (as was done with the Cook-Torrance model in Figure 6). BRDF models which do not include a Fresnel term must be modified in order for them to be compared to the Fresnel based virtual standard. This is most easily done by scaling the sample BRDF by the Fresnel reflectivity of the standard black glass at the specular angle of the haze or gloss measurement. This technique was used in generating the data for Figures 5 and 6.

Using the 20 degree specular gloss values obtained from the Ward model (Figure 5), an image of tiles with decreasing gloss values was rendered (Figure 7). These tiles, corresponding to 20 degree gloss values of 80, 60, 40, and 20, create the expected near linear correspondence between appearance and gloss value. Similarly, four tiles of increasing haze were rendered (Figure 8) using the 2 degree haze values computed with the Ward model. The BRDF model roughness parameter values were chosen so as to produce 2 degree haze values for these tiles of 10, 60, 110 and 160. The 20 degree gloss of all four tiles are set to 100 by scaling the specular coefficient. This is possible since modifying the specular coefficient changes the magnitude of the light reflection, but not the relative distribution. Gloss is an absolute measure of the specular flux while haze is a ratio of off-specular to specular flux.

### 3 Subsurface Highlights - Flop

In computer graphics the color of an opaque dielectric is typically modeled with Lambertian reflectance; the color is considered constant with respect to the viewing angle. This correlates with the standard methods of color measurement used in industry which are based on the same Lambertian (or near Lambertian) reflectance [31, 9, 13]. These methods use the geometries 0/45, 45/0, 0/diffuse, or diffuse/0, with the first number specifying illumination angle and the second number specifying the detector angle. Measurement of color by a single detector angle is sufficient if there is relatively little angular variation in the object's color (e.g. this is the case with many scattering pigments). However, a single measurement is not sufficient for goniochromatic (color changes with angle) materials such as metallic and pearlescent paints.

Metallic paints are produced by combining metallic platelets with colored particles or dyes in the paint substrate [10, 12]. The platelets are oriented near parallel to the surface so that most of the light is reflected near the specular direction while a small portion is scattered diffusely (due to edge scatter). The colored particles or dyes tint the light through selective absorption resulting in a bright color in the near specular direction falling off to a dark color far away from specular. This change in lightness, which is termed flop (also called flip/flop, two tone, or metallic travel) can be seen in Figure 9. A similar flop phenomenon is also achieved with pearlescent paint by using small flakes of mica coated with thin layers of metal oxide [10, 12, 19, 20] which both reflect and transmit incident light. These thin layered platelets cause interference and thus the flop phenomena in pearlescents involves variation in all three coordinates of the color space rather than simply lightness [8].

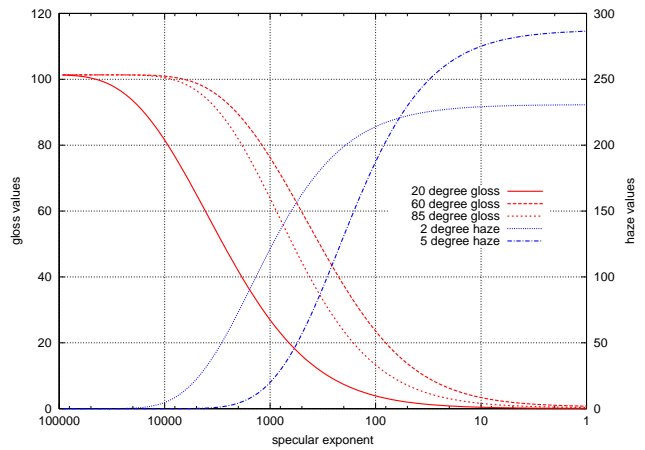


Figure 4: Gloss and haze vs. specular exponent for modified Phong reflection model

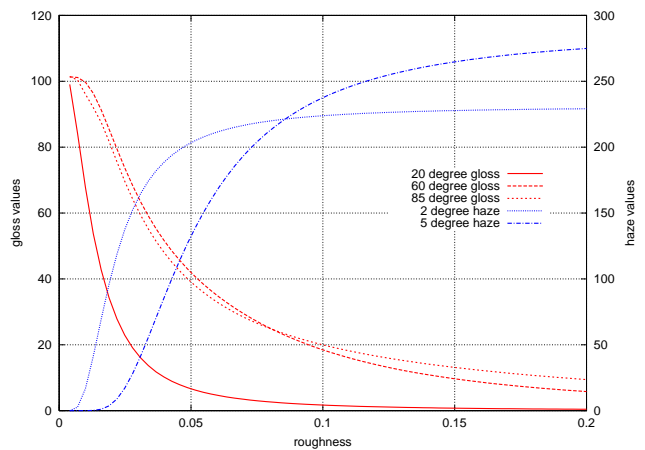


Figure 5: Gloss and haze vs. roughness for Ward isotropic reflection model

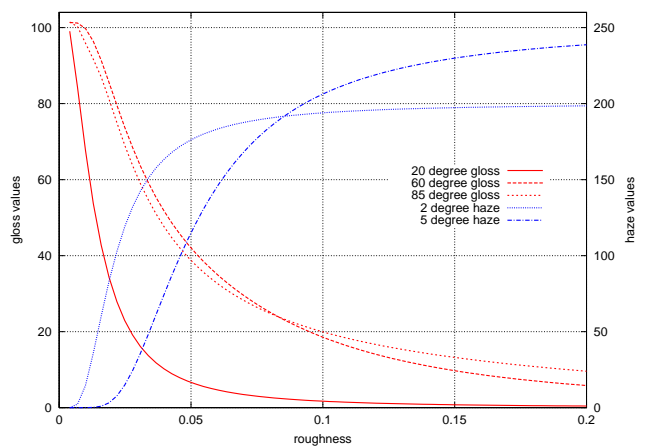


Figure 6: Gloss and haze vs. roughness for Cook-Torrance reflection model

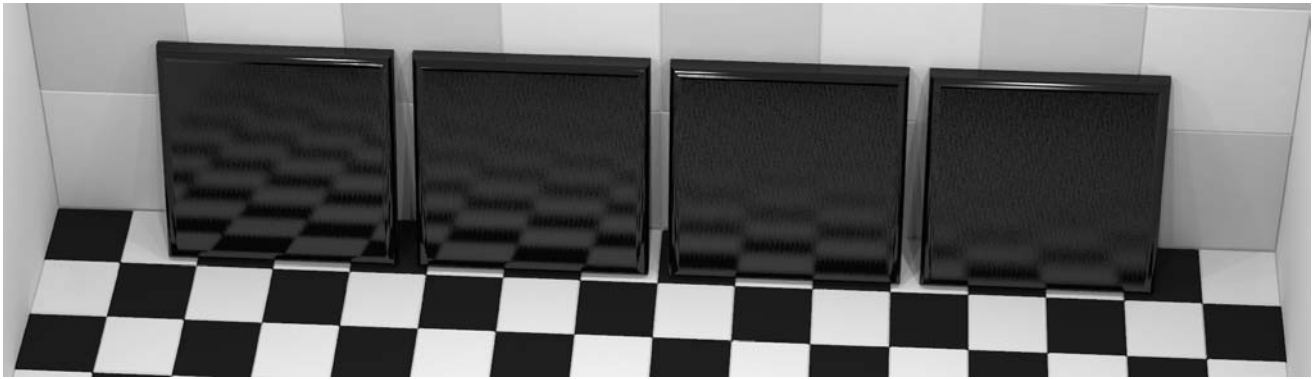


Figure 7: Tiles with measured 20 degree specular gloss values 80, 60, 40, and 20

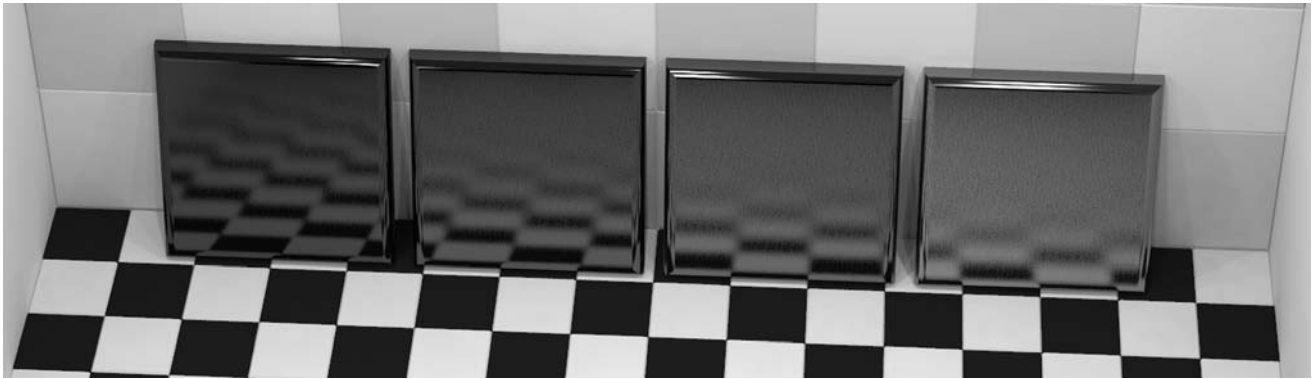


Figure 8: Tiles with measured 2 degree haze values 10, 60, 110, and 160

As mentioned above, a single color measurement is insufficient to characterize the color of goniochromatic material. Much work has been done to determine the measurements required to characterize goniochromatic surfaces. Alman found that three angles are sufficient for characterizing the flop of metallic paints [1]. The paints were illuminated at 45 degrees from normal and were measured at near the specular (15 degrees from specular), far from the specular (110 degrees) and one more measurement in between (45 degrees). Interpolation between these three measurements in CIELAB using a second degree polynomial was found to produce acceptable results. These results were again verified by Rodrigues [34]. Saris, et al. also determined that three similar angular measurements are sufficient for capturing the flop of metallic paints [39]. They compared instrument measurements to human observation and found the best correlation at the angles 25, 45 and 110 degrees from specular with light incident at 45 down from normal. Venable used a more complex exponential based function to interpolate measured XYZ color data from metallic surfaces [42]. He also found that three measurement angles are sufficient to characterize flop and recommended using normal incident illumination measured at 20, 40 and 75 degrees from specular. Interpolation of measured data may also be possible by fitting the data to theoretical models. For example, Bridgeman used radiative heat transfer theory to predict reflection from metallic paint [11]. Additional discussions and comparisons of various metallic paint measurement methods of metallic paints have been presented by Rodrigues [35] and McCamy [28].

Although no standards have as yet been specified, the measurement angles of existing instruments utilized in industry will probably dictate standards. Currently there are working groups in both the American Society for Testing and Materials (ASTM) (sub-committee E12.12, Metallic and Pearlescent Colors) and the

Deutsches Institut für Normung (DIN) which are in the process of discussing final specifications for standard measurements of goniochromatic surfaces [36]. It appears that the ASTM group will accept the DuPont (i.e., Alman) angles of 15, 45 and 110 degrees while the DIN will likely use 25, 45 and 75 degrees [9, 37]. The three required angles of measurement have been assigned the terms near-specular, face, and flop corresponding to the increasing specular angles of the three measurements [5]. Common to both of the proposed standards is the sufficiency of three angles of measurement and the use of the 0/45 measurement (previously existing in CIE color measurement standards) for the face measurement.

Pearlescent and other effects paints present more difficulty because of the additional angular dependency of chroma and hue as well as lightness. Rodrigues showed that the original Alman model can be used to measure and interpolate  $a^*$  and  $b^*$  values in addition to  $L^*$  values using CIELAB [34]. Rösler used illumination at four angles from specular but also allowed for surface tilt in three positions to provide a total of twelve aspectual angles [38]. He found that for many surfaces (e.g. metallics) three or four measurements are sufficient. However for more complex interference and effects surfaces, Rösler emphasized that more measurement angles are possibly required. Another ASTM sub-committee (E12.14, Multidimensional Characterization of Appearance) is interested in developing instrumental and visual standards for multidimensional goniochromatic surfaces. Results from this group are still pending.

Examples of measurements taken from the six metallic paint samples in Figure 14 are shown in Figures 9, 10, and 11. The  $L^*$ ,  $a^*$ , and  $b^*$  values were acquired at the five common aspectual angles of 15, 25, 45, 75, and 110 degrees. The data is easily interpolated using a second degree polynomial of best fit as recommended by Alman. The curves are clamped at the zero point of the

first derivative to ensure monotonicity.

In order to synthesize a picture of these paint samples, a BRDF must be constructed from the data set shown in Figures 9, 10, and 11. The BRDF is the ratio of differential radiance to differential irradiance for a given incident and reflected direction at a given frequency of light:

$$\rho(\Theta_i; \Theta_r; \lambda) = \frac{dL(\Theta_i; \Theta_r; \lambda)}{dE(\Theta_i; \lambda)}. \quad (14)$$

The scale of this ratio generally determines a color's lightness while hue and saturation are the result of the BRDF's variance with respect to the wavelength of light.

In the absence of spectral data, a tristimulus version of the BRDF must be constructed:

$$\rho_R(\Theta_i; \Theta_r) = \frac{R(\Theta_i; \Theta_r)}{\pi R_{max}} \quad (15)$$

$$\rho_G(\Theta_i; \Theta_r) = \frac{G(\Theta_i; \Theta_r)}{\pi G_{max}} \quad (16)$$

$$\rho_B(\Theta_i; \Theta_r) = \frac{B(\Theta_i; \Theta_r)}{\pi B_{max}} \quad (17)$$

where  $R$ ,  $G$ , and  $B$  are the transformed  $L^*$ ,  $a^*$ , and  $b^*$  values in a specific  $RGB$  primary system and where  $R_{max}$ ,  $G_{max}$ , and  $B_{max}$  are the maximum<sup>1</sup> values assigned to the  $RGB$  color scale. The denominator values scale the BRDFs so that direct reflectance of the reference light source off a perfect diffuser results in a computed BRDF of  $1/\pi$  for all three color channels. For light that travels directly from the light source to the object and on to the synthetic camera, a scene which utilizes only tristimulus values for source and material reflectance will result in the same final tristimulus values as one which incorporates the full spectral representation throughout.

This method has its limitations. In particular, significant inter-reflections between surfaces with high spectral variability should be avoided. This also applies to self reflection, so convex objects are preferable. Reflection off gray surfaces (equal energy at all wavelengths) will not produce any difference between the two representations. It is also important to realize that the spectrum of the source is bound at the point of its conversion to tristimulus values. In order to utilize a light source with a different spectral distribution, the tristimulus values must be recalculated or remeasured.

When applied to the determination of the BRDF of metallic or pearlescent paints, the rather daunting task of measuring the tristimulus values at all possible incident and reflected directions as required by (15) through (17) is greatly simplified by using Alman's method. As described above, Alman proposed the measurement of those surfaces at three critical aspect angles (i.e., near-specular, face, and flop) with interpolation at other angles performed in CIELAB space. Although Alman's original work was related to measurement and interpolation within the plane of incidence, good results have been achieved by extending this to measurements out of plane, defining the aspect angle to be

$$\theta_\alpha = \text{acos}((\Theta_i - 2(\Theta_i \cdot \hat{n})) \cdot \Theta_r),$$

the angle between the reflected and specular directions. Thus the four spatial dimensions of the BRDFs presented in (15) through

<sup>1</sup>Colorimetry is typically defined for Lambertian surfaces. The maximum value is defined as the value obtained by direct reflection of the reference light source off a perfect diffuser. Clearly this maximum value can be exceeded in the context of a non-Lambertian surface, where the BRDF value can approach infinity.

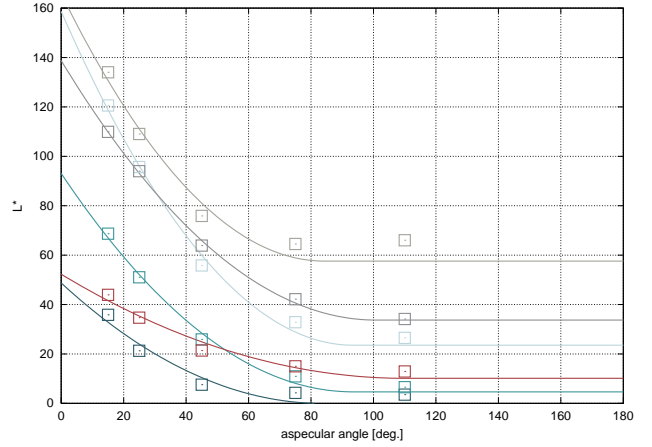


Figure 9:  $L^*$  values vs. aspect angle for the metallic paint samples shown in Figure 14

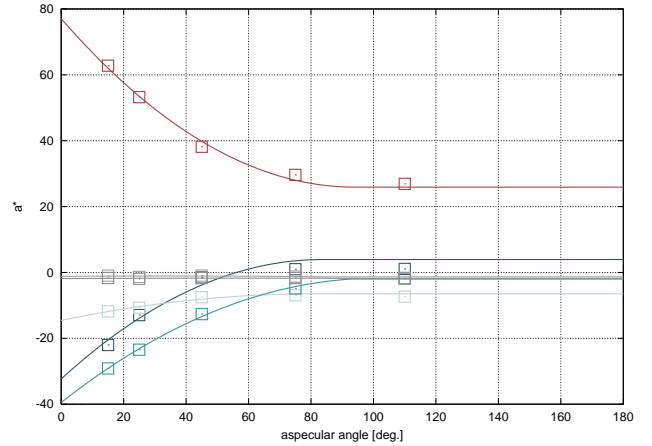


Figure 10:  $a^*$  values vs. aspect angle for the metallic paint samples shown in Figure 14

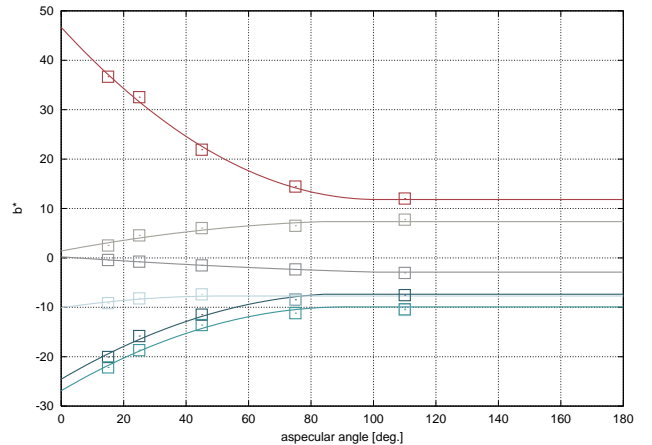


Figure 11:  $b^*$  values vs. aspect angle for the metallic paint samples shown in Figure 14

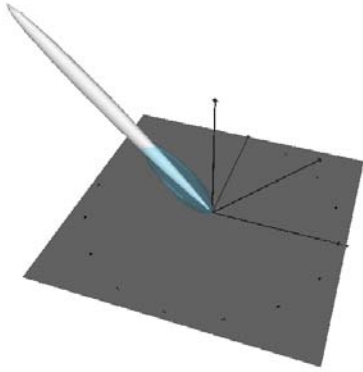


Figure 12: BRDF for a light blue metallic paint combined with a BRDF for a surface with 20 degree specular gloss of 10.

(17) can be reduced to one:

$$\rho_R(\Theta_i; \Theta_r) = \rho_R(\theta_\alpha) = \frac{R(\theta_\alpha)}{\pi R_{max}} \quad (18)$$

$$\rho_G(\Theta_i; \Theta_r) = \rho_G(\theta_\alpha) = \frac{G(\theta_\alpha)}{\pi G_{max}} \quad (19)$$

$$\rho_B(\Theta_i; \Theta_r) = \rho_B(\theta_\alpha) = \frac{B(\theta_\alpha)}{\pi B_{max}}. \quad (20)$$

A picture of such a BRDF for a light blue metallic paint is shown in Figure 12.

An image (Figure 13) of three vases modeled with the computed metallic BRDFs was rendered, using a modified shader, in Radiance [25]. The data for the three vases was taken from Figures 9 to 11. The expected change in lightness is readily apparent on the surface of the vases, giving them a strong sense of metallic reflection. The result is comparable to that found in [41] even though a spectrogoniophotometer was not used to measure the surface reflection.

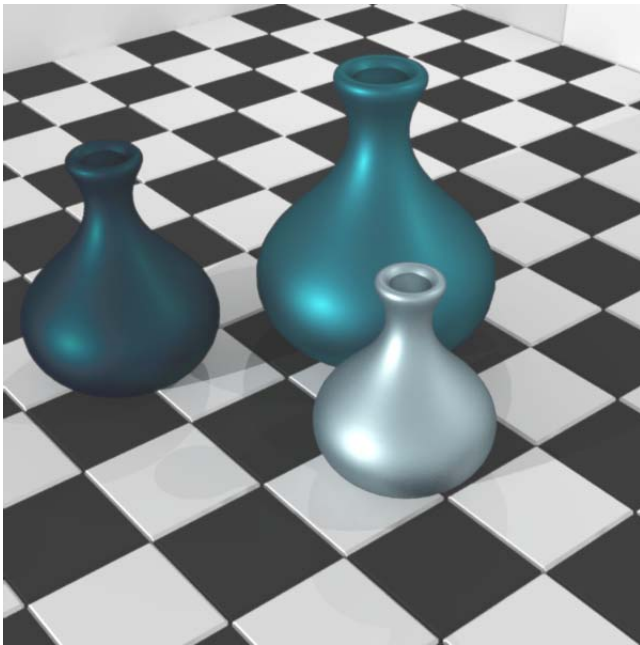


Figure 13: Three vases with metallic paint but no clear coat



Figure 14: Photograph of clear coat finish on metallic paint

## 4 Combining First Surface and Flop

The two most important components of the appearance of an object are its color and gloss. The above discussion provides a means of obtaining gloss and color values using tested and reliable measurements. These two attributes can then be combined to produce a more convincing synthetic image.

Consider the paint samples shown in Figure 14, each paint sample consists of metallic paint covered by a clear coat finish. Light incident on the surface is first scattered by the clear coat resulting in a perceived gloss of some measurable value. The remaining light enters the surface and some of this is reflected out based on the measurable flop values. Here we make the simplifying assumption that the total BRDF can be obtained by simple summation of the first surface and subsurface reflectances:

$$\rho = \rho_{fs} + \rho_{ss}.$$

Figure 15 shows vases modeled with the measured subsurface reflectance of metallic paint along with a first surface of perfectly reflecting ( $G = 100$ ) clearcoat finish. The image of Figure 16 is rendered using a first surface reflection with a 20 degree specular gloss of 10 and 60. The BRDF used for the shell with gloss of 10 is shown in Figure 12. The first surface is achieved by using the Ward reflection model with surface roughness chosen to produce the particular gloss values. The data for the vases and shells in Figures 15 and 16 were taken from Figures 9 to 11.

## 5 Conclusion

Standard appearance scales, such as gloss and haze, can be used to set the parameters of existing computer graphics reflection models. An advantage to this approach is that it lets the user of these models work with terms that correspond to the effect that these terms have on the appearance of the rendered object. This is far more intuitive than adjusting the specular exponent in the Phong model or the surface roughness in the Ward or Cook-Torrance models. In addition, paint and coatings experts have attempted to give these appearance scales a psychophysical component so, for example, there is a uniform change in gloss as it increases from 0 to 100.

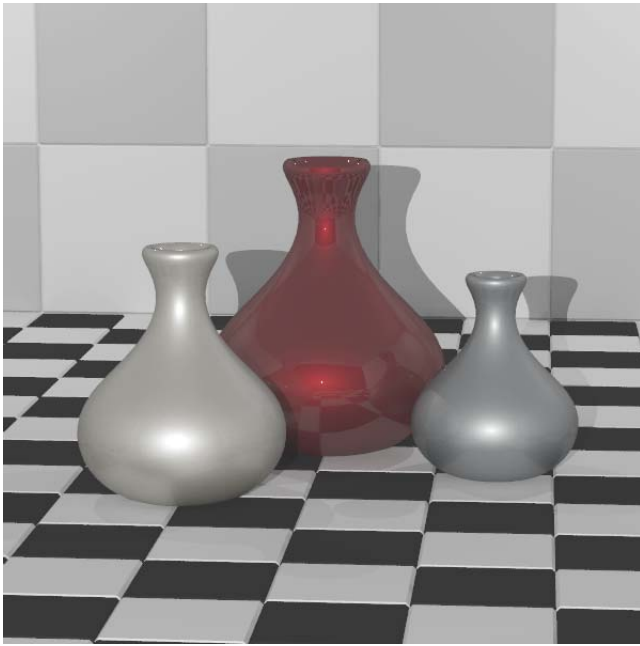


Figure 15: Three vases with metallic paint and a first surface of gloss 100

The values to be employed for gloss and haze in the reflection models can be determined using inexpensive measurement instruments. This makes it possible to model the appearance of an existing object by making a few simple measurements. In the majority of appearance applications, the expense of a spectrogoniophotometer and the full generality of a BRDF are not required. A surface as complex as a metallic or pearlescent automotive finish can be rendered using as few as four data values: one gloss measurement in the specular direction and colorimetric measurements in three critical aspecular directions.

The use of standard appearance scales makes it possible to produce equivalent renderings using two different surface reflection models. For example, the Phong model, which is built into the OpenGL standard, could be used in an interactive program to select the gloss for a surface. This value for gloss could then subsequently be used in an offline rendering system that employs the Cook-Torrance reflection model. The appearance of the rendered objects would be comparable even though the reflection models employed were different. This is similar to using CIE tristimulus values to achieve the same object color from two different image synthesis programs.

Finally, there is a rich symbiotic relationship that exists between the appearance industry and the field of computer graphics. The use of standard appearance scales to set the parameters of reflection models makes it easier for appearance professionals to employ computer graphics in their work. This may eventually lead to a set of computer-aided color appearance design tools similar to the computer-aided geometric design tools that have been used in automotive and aircraft companies for thirty years [29]. There is also much that the computer graphics community can learn from the color appearance discipline. A century of experience in controlling real world appearance is clearly relevant to our comparatively recent attempts to design and render synthetic environments.

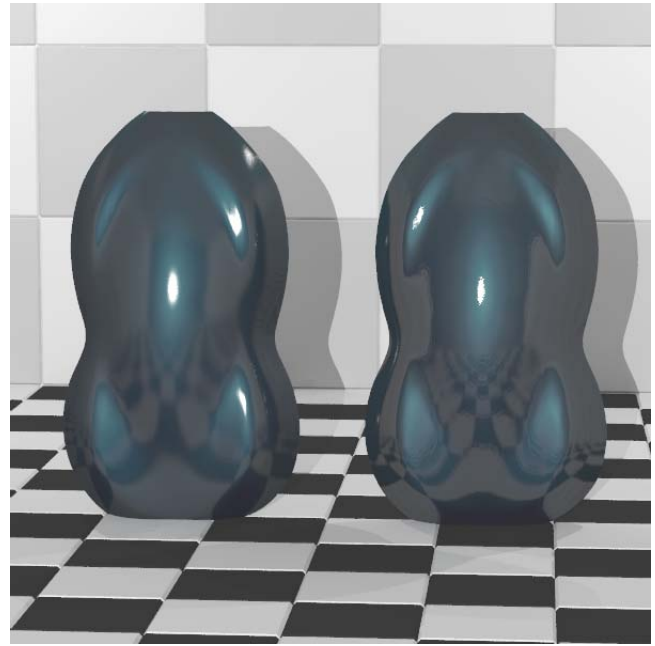


Figure 16: Two automotive shells with 20 degree specular gloss of 10 and 60

## 6 Acknowledgments

The authors would like to thank DuPont Automotive Products for providing paint samples and reflectance measurements. This work was funded by the National Institutes of Standards and Technology.

## References

- [1] David H. Alman. Directional color measurement of metallic flake finishes. In *Proceedings of the ISCC Williamsburg Conference on Appearance*, pages 53–56, 1987.
- [2] *Annual Book of ASTM Standards*, volume 06.01. American Society for Testing and Materials, Philadelphia, PA, 1999.
- [3] *ASTM D 4039-93, Standard Test Method for Reflection Haze of High-Gloss Surfaces*. Volume 06.01 of Annual Book of ASTM Standards [2], 1999.
- [4] *ASTM D 523-89, Standard Test Method for Specular Gloss*. Volume 06.01 of Annual Book of ASTM Standards [2], 1999.
- [5] *ASTM E 284-99a, Standard Terminology of Appearance*. Volume 06.01 of Annual Book of ASTM Standards [2], 1999.
- [6] *ASTM E 430-97, Standard Test Methods for measurement of Gloss of High-Gloss Surfaces by Goniophotometry*. Volume 06.01 of Annual Book of ASTM Standards [2], 1999.
- [7] Association Internationale de la Couleur (AIC). *Mondial Couleur 85, Proceeding of the 5th Congress of The International Color Association*, Paris, France, 1985.
- [8] Gorow Baba. Gonio-spectrophotometric analysis of pearl-mica paint. *Die Farbe*, 37:99–110, 1990.
- [9] Roy S. Berns. *Billmeyer and Saltzman's Principles of Color Technology*. John Wiley & Sons, Inc., New York, 3rd edition, 2000.

- [10] Robert Besold. Metallic effect - characterization, parameter and methods for instrumentally determination. *Die Farbe*, 37:79–85, 1990.
- [11] Tony Bridgeman. The reflection of metallic paints. In Association Internationale de la Colour [7]. Article No. 5.
- [12] Gunter Buxbaum, editor. *Industrial Inorganic Pigments*. Weinheim, New York, 1993.
- [13] *Colorimetry*. Commission Internationale de L'eclairage, 2nd edition, 1986. Publication 15.2.
- [14] Robert L. Cook and Kenneth E. Torrance. A reflectance model for computer graphics. *ACM Transactions on Graphics*, 1:7–24, 1982.
- [15] Ronald Cools, Dirk Laurie, and Luc Pluym. Cubpack++. software: Numerical cubature class library. <ftp://ftp.cs.kuleuven.ac.be/pub/NumAnal-AppMath/Cubpack/all.tar.gz>, Accessed November 10, 2000.
- [16] Ronald Cools, Dirk Laurie, and Luc Pluym. Cubpack++. <http://www.cs.kuleuven.ac.be/nines/research/cubpack/>, Accessed November 10, 2000.
- [17] Ronald Cools, Dirk Laurie, and Luc Pluym. Algorithm 764: Cubpack++ - a C++ package for automatic two-dimensional cubature. *ACM Transactions on Mathematical Software*, 23:1–15, 1997.
- [18] Ronald Cools, Dirk Laurie, and Luc Pluym. A user manual for Cubpack++. Technical Report TW 255, Katholieke Universiteit Leuven, Department of Computer Science, Leuven, Belgium, 1997. Version 1.1.
- [19] Klaus-Dieter Franz. High luster mica pigments for automotive coatings. In Association Internationale de la Colour [7]. Article 70.
- [20] Franz Hofmeister. Colourimetric evaluation of pearlescent pigments. In Association Internationale de la Colour [7]. Article 74.
- [21] Richard S. Hunter. Methods of determining gloss. *Journal of Research, NBS*, 17:77, 281, 1937. NBS Research Paper, RP 958.
- [22] Richard S. Hunter and Richard W. Harold. *The Measurement of Appearance*. John Wiley and Sons, Inc., New York, second edition, 1987.
- [23] Richard S. Hunter and Dean B. Judd. Development of a method of classifying paints according to gloss. *ASTM Bulletin*, (97):11, March 1939.
- [24] James T. Kajiya. The rendering equation. In *Computer Graphics, Annual Conference Series*, pages 143–150. ACM SIGGRAPH, 1986.
- [25] Greg Ward Larson and Rob Shakespeare. *Rendering with Radiance. The Art and Science of Lighting Visualization*. Morgan Kaufmann Publishers, Inc., San Francisco, 1998.
- [26] Gregory J. Ward Larson. Measuring and modeling anisotropic reflection. *Computer Graphics (Proceedings of SIGGRAPH 92)*, 26(2):265–272, July 1992.
- [27] Robert Lewis. Making shaders more physically plausible. *Fourth Eurographics Workshop on Rendering*, pages 47–62, June 1993.
- [28] C. S. McCamy. Observation and measurement of appearance of metallic materials. part I. macro appearance. *Color Research and Application*, 21(4), 1996.
- [29] Gary W. Meyer. Computer aided color appearance design. *Proceedings of the First International Conference on Color in Graphics and Image Processing*, 2000.
- [30] F. E. Nicodemus, J. C. Richmond, J. J. Hsia, I. W. Ginsberg, and T. Limperis. Geometric considerations and nomenclature for reflectance. Technical Report MN-160, U.S. Department of Commerce, National Bureau of Standards, October 1977.
- [31] ASTM Committee E-12 on Appearance of Materials. *ASTM standards on color and appearance measurement*. American Society for Testing and Materials, Philadelphia, PA, sixth edition, 1996.
- [32] Fabio Pellacini, James A. Ferwerda, and Donald P. Greenberg. Toward a psychophysically-based light reflection model for image synthesis. In *Computer Graphics, Annual Conference Series*, pages 55–64. ACM SIGGRAPH, 2000.
- [33] Bui-T. Phong. Illumination for computer generated pictures. *Communications of the ACM*, 18(6):311–317, June 1975.
- [34] Allan B. J. Rodrigues. Color vision in instrumental color matching. *16th International Conference in Organic Coatings*, 1990.
- [35] Allan B. J. Rodrigues. Measurement of metallic and pearlescent colors. *Die Farbe*, 37:65–78, 1990.
- [36] Allan B. J. Rodrigues. Color and appearance measurement of metallic and pearlescent finishes. *ASTM Standardization News*, 23(10):68–72, 1995.
- [37] Allan B. J. Rodrigues and Larry E. Steenhoek. Astm e-12.12: Measurement of metallic and pearlescent colors. *Die Farbe*, 42(4/6):151–158, 1996.
- [38] Gerhard Rösler. Multigeometry color measurements of effect surfaces. *Die Farbe*, 37:111–121, 1990.
- [39] H. J. A. Saris, R.J.B. Gottenbos, and H. van Houwelingen. Correlation between visual and instrumental colour differences of metallic paint films. *Color Research and Application*, 15(4), 1990.
- [40] Peter Shirley, Helen Hu, Brian Smits, and Eric P. Lafortune. A practitioners' assessment of light reflection models. *Pacific Graphics '97*, October 1997.
- [41] Atsushi Takagi, Hitoshi Takaoka, Tetsuya Oshima, and Yoshinori Ogata. Accurate rendering technique based on colorimetric conception. In *Computer Graphics, Annual Conference Series*, pages 263–272. ACM SIGGRAPH, 1990.
- [42] William H. Venable. A model for interpreting three-angle measurements of flake finishes. In *Proceedings of the ISCC Williamsburg Conference on Appearance*, pages 57–60, 1987.